

Two types of phase diagrams for two-species Bose-Einstein condensates

Z. B. Li¹, Y. M. Liu^{2,3}, D. X. Yao¹, and C. G. Bao¹

¹*State Key Laboratory of Optoelectronic Materials and Technologies,*

School of Physics, Sun Yat-Sen University, Guangzhou, 510275, P. R. China

²*Department of Physics, Shaoguan University, Shaoguan, 512005, P. R. China and*

³*State Key Laboratory of Theoretical Physics, Institute of Theoretical Physics, Chinese Academy of Sciences, Beijing, 100190, China*

Under the Thomas-Fermi approximation, a relatively much simpler analytical solutions of the coupled Gross-Pitaevskii equations for the two-species BEC have been derived. Additionally, a model for the asymmetric states has been proposed, and the competition between the symmetric and asymmetric states has been evaluated. The whole parameter-space is divided into zones, each supports a specific phase, namely, the symmetric miscible phase, the symmetric immiscible phase, or the asymmetric phase. Based on the division the phase-diagrams against any set of parameters can be plotted. Thereby, the effects of these parameters can be visualized. There are three critical values in the inter-species interaction V_{AB} and one in the ratio of particle numbers N_A/N_B . They govern the transitions between the phases. Two cases, (i) the repulsive V_{AB} matches the repulsive $V_A + V_B$, and (ii) the attractive V_{AB} nearly cancels the effect of the repulsive $V_A + V_B$ have been particularly taken into account. The former leads to a complete separation of the two kinds of atoms, while the latter lead to a collapse. Finally, based on an equation derived in the paper, a convenient experimental approach is proposed to determine the ratio of particle numbers.

PACS numbers: 03.75.Mn, 03.75.Kk

*Correspondence to stsbcg@mail.sysu.edu.cn

I. INTRODUCTION

There is increasing interest in two-species Bose-Einstein condensate (TBEC) in last two decades since it was first studied theoretically by Ho and Shenoy[1], and was achieved experimentally by Myatt, et al.[2]. The TBEC provides an important tool to clarify the inter-species and intra-species interactions. Besides, molecules in well defined rovibrational levels with permanent electric-dipole moment can be thereby obtained, and they are valuable for studying the strongly interacting quantum gases.[3–6]. Experimentally, the Rb-Cs mixture has been realized via a magnetic trap [7] or an optical trap [8]. The Rb-Yb mixture has been realized via a combined magneto-optical trap [9]. The K-Rb, Na-Rb, Sr-Rb and the isotopic mixtures ⁸⁷Rb-⁸⁵Rb, ¹⁶⁸Yb-¹⁷⁴Yb, ⁸⁴Sr-⁸⁶Sr, and ⁸⁶Sr-⁸⁸Sr have also been realized and studied recently (refer to the references listed in [10]).

There are a number of theoretical literatures dedicated to the TBEC [1, 11–28]. The ground state (g.s.) is found to have three phases, symmetric miscible phase, symmetric immiscible phase, and asymmetric immiscible phase, depending on the parameters. There are a number of parameters (the strengths of the intra- and inter-species interactions, the particle numbers, the masses of atoms, and those for the trap) affecting the behavior of the system. To clarify the effects of them is a main topic of study.

This paper is dedicated to obtain the phase-diagrams. How the spatial configuration of the g.s. is affected by the parameters can be thereby visualized. For this pur-

pose, effort is made to divide the whole parameter-space into zones, each supports a specific spatial configuration. Based on the division, two types of phase-diagrams are plotted. Related analysis is supported by analytical formalism. The emphasis is placed on the qualitative aspect. The particle numbers are considered to be large ($\geq 10^4$) so that the Thomas-Fermi approximation (TFA) can be applied. The symmetric states are obtained by solving the coupled Gross-Pitaevskii equations (CGP) in an analytical way. Whereas the asymmetric states are obtained by introducing a model. Both repulsive and attractive inter-species interactions are considered. Two critical cases, namely, (i) the repulsive inter-species interaction matches the repulsive intra-species interaction and (ii) the attractive inter-species interaction nearly cancels the repulsive intra-species interaction, are taken into account.

II. SYMMETRIC GROUND STATE

There are N_A A-atoms with mass m_A and interacting via $V_A = c_A \sum_{i<i'} \delta(\mathbf{r}_i - \mathbf{r}_{i'})$, and N_B B-atoms with mass m_B and $V_B = c_B \sum_{j<j'} \delta(\mathbf{r}_j - \mathbf{r}_{j'})$. The A- and B-atoms are interacting via $V_{AB} = c_{AB} \sum_{i<j} \delta(\mathbf{r}_i - \mathbf{r}_j)$. Their spin-degrees of freedom are considered as being frozen. They are trapped by the isotropic parabolic potentials $\frac{1}{2} m_S \omega_S^2 r^2$ ($S = A$ or B). In the g.s. Ψ_{gs} the atoms of the same kind will have the same wave function ϕ_S which is most advantageous to binding. Thus,

$$\Psi_{gs} = \prod_{j=1}^{N_A} \phi_A(\mathbf{r}_j) \prod_{k=1}^{N_B} \phi_B(\mathbf{r}_k) \quad (1)$$

It is well known that Ψ_{gs} and the trap might not have the same symmetry. When the interspecies interaction is

sufficiently repulsive, the two kinds of atoms might separate from each other in an asymmetric way. Nonetheless, we consider first the case that the g.s. is symmetric.

In this case, let $\phi_A(\mathbf{r}_j) \equiv \frac{u(r_j)}{\sqrt{4\pi r_j}}$ and $\phi_B(\mathbf{r}_k) \equiv \frac{v(r_k)}{\sqrt{4\pi r_k}}$. We introduce a mass m and a frequency ω . $\hbar\omega$ and $\sqrt{\hbar/(m\omega)}$ are used as units for energy and length in this paper. We further introduce $\gamma_s \equiv \frac{m_s(\omega_s)}{m}$ and a set of parameters $\alpha_1 \equiv N_{ACA}/(4\pi\gamma_A)$, $\beta_1 \equiv N_{BCAB}/(4\pi\gamma_A)$, $\alpha_2 \equiv N_{BCB}/(4\pi\gamma_B)$, $\beta_2 \equiv N_{ACAB}/(4\pi\gamma_B)$. This set is called the weighted strengths (W-strengths). Under the TFA, the CGP for u and v appear as

$$\left(\frac{r^2}{2} + \alpha_1 \frac{u^2}{r^2} + \beta_1 \frac{v^2}{r^2} - \varepsilon_1\right)u = 0 \quad (2)$$

$$\left(\frac{r^2}{2} + \beta_2 \frac{u^2}{r^2} + \alpha_2 \frac{v^2}{r^2} - \varepsilon_2\right)v = 0 \quad (3)$$

where β_2 and β_1 for the inter-species interaction have the same sign (+ or -) while α_2 and α_1 for the intra-species interaction are considered to be positive only. The chemical potential for the A-atoms (B-atoms) is equal to $\gamma_A\varepsilon_1$ ($\gamma_B\varepsilon_2$). The normalization $\int u^2 dr = 1$ and $\int v^2 dr = 1$ are required. $u \geq 0$ and $v \geq 0$ are safely assumed.

Eqs.(2,3) demonstrate that the combined effects of the nine dynamical parameters c_S , c_{AB} , N_S , m_S , and ω_S ($S = A$ and B) are sufficiently embodied by the four W-strengths. Thus an approach based on the W-strengths would lead to a simplification. Based on the W-strengths, we define

$$Y_1 \equiv (\alpha_2 - \beta_1)/(2\alpha) \quad (4)$$

$$Y_2 \equiv (\alpha_1 - \beta_2)/(2\alpha) \quad (5)$$

where $\alpha \equiv \alpha_1\alpha_2 - \beta_1\beta_2$. Y_1 and Y_2 are crucial in constituting the solutions of the CGP as shown below.

It has been known that the spatial configuration of the symmetric g.s. has two phases. When each kind of atoms form a core surrounding the center, then it is named miscible phase denoted as (A,B) (if the B-atoms have a broader distribution) or (B,A). When a kind of atoms form a core while the other kind form a shell away from the center, it is named immiscible phase denoted as [A-B] (if the B-atoms form the shell) or [B-A]. More strictly, the miscible phase has both $u/r|_{r=0}$ and $v/r|_{r=0}$ being nonzero, while the immiscible phase has one of them being zero.

The analytical solutions of the symmetric g.s. under the TFA have been worked out previously [16, 28]. Nonetheless, in terms of the W-strengths, the analytical solutions could have a considerably simpler form. This simplification is valuable because it substantially benefits a more detailed analysis. Thus, the simplified solutions are given in the Appendix. Besides, the division of the whole parameter-space into zones is a crucial point in our paper and is also included in the Appendix. With the division, various types of phase-diagrams can be plotted.

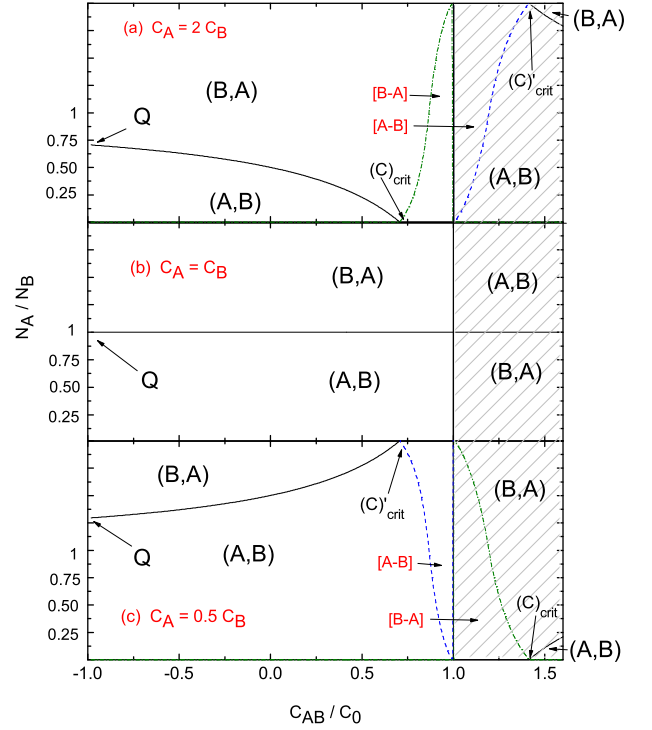


FIG. 1: (Color online) The phase diagram with respect to C_{AB}/C_0 and N_A/N_B , where $C_0 \equiv \sqrt{C_A C_B}$. $\gamma_A = \gamma_B = 1$, $N_B = 10^4$, $C_B = 10^{-3}$, and C_A is given at three values marked in the panels. The units $\hbar\omega$ and $\sqrt{\hbar/(m\omega)}$ are used in this paper. The ordinate y is given from 0 to 2. When $y \leq 1$, $N_A/N_B = y$. When $y > 1$, $N_A/N_B = 1/(2-y)$ (in other words, N_A/N_B is ranged from 0 to ∞). The labels of phase (e.g., (A,B)) are directly marked in the associated zone. The curve separating (A,B) and (B,A) fulfills $Y_1 = Y_2$, at which u and v overlap completely (when $Y_1 = Y_2$, we have $\alpha_2 - \beta_1 = \alpha_1 - \beta_2$, then one can directly prove that $u = v$ is a solution of the CGP). The dash curve separating (A,B) and [A-B] fulfills $X_2 = 0$ (i.e., $(1 + \frac{\alpha_2}{\beta_2})^{2/3} = 2\beta_2 Y_1$, refer to eq.(18)). The dash-dot curve separating (B,A) and [B-A] fulfills $X'_1 = 0$ (i.e., $(1 + \frac{\alpha_1}{\beta_1})^{2/3} = 2\beta_1 Y_2$). The shaded area has $C_{AB} > C_0$ (or $\alpha < 0$) where the g.s. is asymmetric while the symmetric solution of the CGP is a collectively excited metastable state. The point Q marks the limit of $(N_A/N_B)_{crit}$ when $C_{AB} \rightarrow -C_0$.

III. THE PHASE-DIAGRAM AGAINST THE INTERSPECIES INTERACTION AND THE PARTICLE NUMBERS

Based on the analytical solutions of the CGP and the division of the parameter-space which are given in the Appendix, the first type of phase-diagrams are shown in Fig.1 .

Let us define a critical value $(C)_{crit} \equiv \frac{\gamma_A}{\gamma_B} \sqrt{\frac{C_B}{C_A}}$. In Fig.1 the lower and upper ends of the dash-dot curve have $C_{AB}/C_0 = (C)_{crit}$ and 1, respectively. The two ends of the dash curve have $C_{AB}/C_0 = 1$ and $(C')_{crit} \equiv 1/(C)_{crit}$, respectively. Accordingly, C_{AB}/C_0 contains

three critical values $(C)_{crit}$, 1, and $(C)'_{crit}$. In Fig.1a, when $C_{AB}/C_0 \leq -1$, the system collapses (see below). When $-1 < C_{AB}/C_0 \leq (C)_{crit}$, the g.s. is in miscible phase. There is a competition between (A,B) and (B,A) phases depending on N_A/N_B . When N_A is sufficiently small so that $Y_1 \geq Y_2$, then the distribution of the A-atoms will be narrower and the g.s. will be in (A,B) (refer to the Appendix), or vice versa. Thus, from the condition $Y_1 = Y_2$, we can define a critical ratio

$$(N_A/N_B)_{crit} = (C_B\gamma_A - C_{AB}\gamma_B)/(C_A\gamma_B - C_{AB}\gamma_A) \quad (6)$$

When $N_A/N_B < (N_A/N_B)_{crit}$, the g.s. is in (A,B), or otherwise in (B,A). When $N_A/N_B = (N_A/N_B)_{crit}$, the distributions of the A- and B-atoms overlap completely (refer to the Appendix). When $C_{AB}/C_0 \rightarrow -1$, $(N_A/N_B)_{crit} \rightarrow \sqrt{C_B/C_A}$, thus the condition for the g.s. in (A,B) is $N_A/N_B < \sqrt{C_B/C_A}$ (in other words, the (A,B) phase would be more probable if C_A is relatively weak and/or N_A is small). When $C_{AB}/C_0 = (C)_{crit}$, $(N_A/N_B)_{crit} = 0$. When C_{AB} increases further, the (A,B) phase disappears and the A-atoms begin to be distributed more outward. When $(C)_{crit} < C_{AB}/C_0 \leq 1$, There is a competition between the [B-A] and (B,A) phases depending also on N_A/N_B . When N_A is sufficiently small to enable $X'_1 < 0$, the A-atoms will form a shell and the g.s. is in immiscible phase. Otherwise, in miscible phase. When $C_{AB}/C_0 \rightarrow 1$, the zone of [B-A] covers nearly the whole range of N_A/N_B , and thus the immiscible phase becomes dominant. When $1 < C_{AB}/C_0 \leq (C)'_{crit}$, the lowest symmetric solutions of the CGP have the B-atoms being distributed more outward (in [A-B] or (A,B) phases). Nonetheless, when C_{AB} increases and crosses C_0 , a transition from [B-A] to [A-B] will occur. During this transition, the atoms in the shell and in the core interchange their roles (i.e., those in the core jump to the shell, and vice versa). This causes a remarkable increase in energy (as shown below). Accordingly, when $C_{AB}/C_0 \geq 1$, the symmetric configuration is no more stable. For this reason, we shall more concentrate on the case $C_{AB} < C_0$.

When $(C)_{crit} = 1$, $(C)'_{crit}$ also = 1, and the areas of the zones of [B-A] and [A-B] both become zero, and therefore the immiscible phase does not appear (Fig.1b belongs to this case). Thus the difference between C_A/γ_A^2 and C_B/γ_B^2 is a basic requirement for the appearance of the immiscible phase.

For the case $(C)_{crit} > 1$ (Fig.1c belong to this case), a similar discussion can be performed where the A- and B-atoms interchange their roles.

To conclude, in most cases, the g.s. is in miscible phases. There is a critical value $(N_A/N_B)_{crit}$ to judge either (A,B) or (B,A) would win. Besides, there is a critical value $(C)_{crit}$. When $(C)_{crit} < C_{AB}/C_0 < 1$ and when N_A is so small that $X'_1 < 0$, the immiscible [B-A] phase will emerge in the zone lying between the curve $X'_1 = 0$ and the vertical line $C_{AB}/C_0 = 1$ (where $\alpha = 0$). Note that the [B-A] phase requires thIn this zone $Y_2 > 0$

and $Y_1 < 0$ (refer to the Appendix), it implies that the W-strengths should be appropriately given. The condition for [A-B] can be similarly deduced. Thus the zones of the immiscible phase appear only by the two sides of the vertical line $C_{AB}/C_0 = 1$. The area of the zones depends on how far $(C)_{crit}$ deviates from 1. Recall that $(C)_{crit}$ contains the factor $(\omega_A/\omega_B)^2$. Thus the ratio of the two frequencies is a very sensitive factor to affect the spatial configuration (say, a small reduction of ω_A will reduce $(C)_{crit}$, the zone of [B-A] shown in Fig.1a will be thereby broader, and thus favors the A-atoms to form a shell).

The spatial configurations, namely, the patterns of the wave functions have already been plotted in many literatures. To avoid tedious, only two particular cases are plotted here.

- (i) For attractive V_{AB} with $C_{AB} \gtrsim -C_0$

In this case both Y_1 and Y_2 are positive and tend to ∞ . Let us assume $Y_1 > Y_2$. Accordingly, the A-atoms have a narrower distribution. Since the radius of the inner core $r_{in} \propto Y_1^{-1/5}$ (Refer to the Appendix), it tends to zero. On the other hand, the outer border $r_{out} = \sqrt{2\varepsilon_2} = [15(\alpha_2 + \beta_2)]^{1/5}$. When $C_{AB} \rightarrow -C_0$, $\alpha_2 + \beta_2 \rightarrow \frac{N_B C_0}{4\pi\gamma_B} (\sqrt{\frac{C_B}{C_A}} - \frac{N_A}{N_B})$. Recall that $\sqrt{\frac{C_B}{C_A}}$ is the limit of $(N_A/N_B)_{crit}$ when $C_{AB} \rightarrow -C_0$. Thus, if N_A/N_B is so given that it would considerably smaller than the limit, then r_{out} would be finite while $r_{in} \rightarrow 0$. In this case, we will have a very dense core together with a thin tail extending outward formed by the B-atoms. Alternatively, if the W-strengths are so given that $Y_1 < Y_2$, then the tail is formed by the A-atoms. Whereas, when $\frac{N_A}{N_B} \rightarrow \sqrt{\frac{C_B}{C_A}}$, the tail disappears and all the atoms stay inside a very small core. Numerical calculations support this suggestion as shown in Fig.2, where the tail is long in 2a and 2b, but very short in 2c. The extremely high density at the center implies that the system tends to collapse.

- (ii) For repulsive V_{AB} with $C_{AB} \lesssim C_0$

When $C_{AB} \rightarrow C_0$, the two species tend to separate completely from each other (refer to the Appendix). Examples for the cases with $C_{AB} = 0.99C_0$ are given in Fig.3 characterized by having a shell attached to the outward border of a core. In Fig.3 N_B remains unchanged, while the increase of N_A pushes the shell of the B-atoms more and more outward.

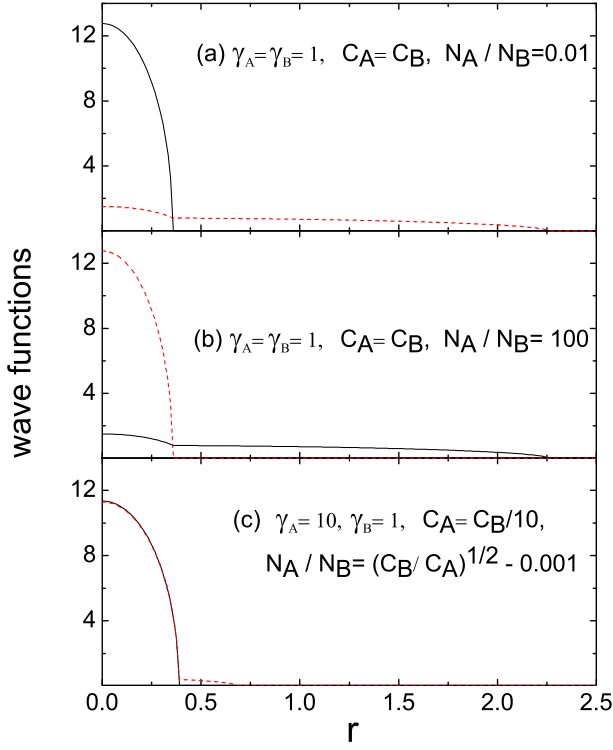


FIG. 2: (Color online) u/r (solid) v/r (dash) against r (in $\sqrt{\hbar/(m\omega)}$) when the attraction from V_{AB} nearly cancels the repulsion from the intra-species interaction ($C_{AB} = -0.99C_0$ is given). $N = N_A + N_B = 5 \times 10^4$, $C_B = 10^{-3}$, the other parameters are marked in the panels. In addition to the high density at the center, there is a long tail of B-atoms, a long tail of A-atoms, and a very short tail in a, b, and c.

IV. TOTAL ENERGY AND THE COMPETITION OF SYMMETRIC AND ASYMMETRIC STATES

When ϕ_A and ϕ_B have been known, the total energy of the system (neglecting the kinetic energy) is

$$E = \frac{N_A}{2} \langle r^2 \rangle_A + \frac{N_B}{2} \langle r^2 \rangle_B + \frac{N_A^2}{2} V_A \langle \phi_A^2 \rangle_A + \frac{N_B^2}{2} V_B \langle \phi_B^2 \rangle_B + N_A N_B V_{AB} \langle \phi_A^2 \rangle_B \quad (7)$$

where $\langle r^2 \rangle_A = \int \phi_A^2 r^2 d\mathbf{r}$, $\langle \phi_A^2 \rangle_A = \int \phi_A^4 d\mathbf{r}$, $\langle \phi_A^2 \rangle_B = \langle \phi_B^2 \rangle_A = \int \phi_A^2 \phi_B^2 d\mathbf{r}$, and so on.

Examples of E/N (where $N = N_A + N_B$) are plotted in Fig.4. Where the five curves for symmetric states goes up with C_{AB} as expected. In all cases there is a notable jump when C_{AB} increases and crosses C_0 (strictly, only the case that C_{AB} tends to $\pm C_0$ can be calculated). This jump is associated with the transition from $[A - B]$ to $[B - A]$ mentioned above. This figure demonstrates that the increase of energy in the jump can be quite large. It implies that very high-lying collectively excited states might exist. All the horizontal lines are for asymmetric states, they are obtained via a model shown below.

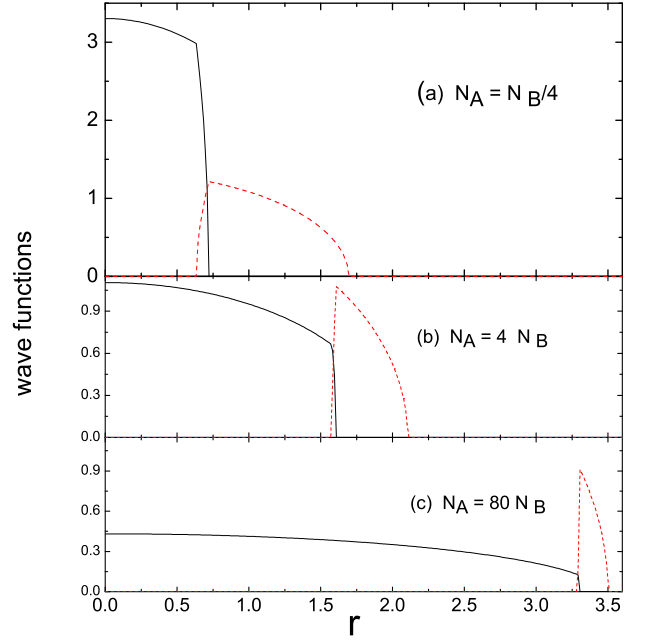


FIG. 3: (Color online) u/r (solid) v/r (dash) against r (in $\sqrt{\hbar/(m\omega)}$) when the repulsion from V_{AB} matches the repulsion from V_A and V_B ($C_{AB} = 0.99C_0$ is given). The other parameters are $\gamma_A = \gamma_B = 1$, $N_B = 10^4$, $C_B = 10^{-3}$, and $C_A = C_B/2$. N_A is marked in each panel.

Let z and r_\perp ($z^2 + r_\perp^2 = r^2$) be the axial coordinates, and two parameters z_o and r_o are introduced. Then, it is assumed that when $-r_o \leq z \leq z_o$

$$u = \frac{1}{c} r \sqrt{1 - r^2/r_o^2} \quad (8)$$

$$v = 0 \quad (9)$$

and when $z_o < z \leq r_o$

$$u = 0 \quad (10)$$

$$v = \frac{1}{d} r \sqrt{1 - r^2/r_o^2}. \quad (11)$$

In other words, we have proposed a model in which a ball with radius r_o is divided into two sides separated by the plane $z = z_o$. The A-atoms and B-atoms stay separately in the two sides. The orientation of the Z-axis is irrelevant (because the trap is isotropic). From the normalization, we have

$$c^2 = \frac{1}{15} r_o^3 + \frac{1}{8} r_o^2 z_o - \frac{1}{12} z_o^3 + \frac{1}{40} r_o^{-2} z_o^5 \quad (12)$$

$$d^2 = \frac{1}{15} r_o^3 - \frac{1}{8} r_o^2 z_o + \frac{1}{12} z_o^3 - \frac{1}{40} r_o^{-2} z_o^5 \quad (13)$$

The two parameters r_o and z_o are determined by minimizing the total energy E (which is calculated via eq.(7) where the contribution from the kinetic energy has been neglected). The resultant E/N are plotted in Fig.4 and they appear as horizontal lines. In various cases, due

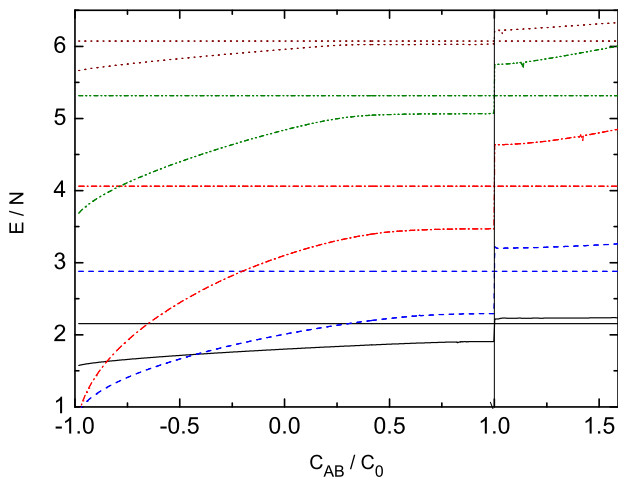


FIG. 4: (Color online) E/N (in $\hbar\omega$) of the lowest symmetric and asymmetric states against C_{AB}/C_0 . The latter are given by horizontal lines, while the former are noisy. The parameters are given as $\gamma_A = 5$, $\gamma_B = 1$, $N = N_A + N_B = 5 \times 10^4$, $C_B = 10^{-3}$, and $C_A = 2C_B$. The solid, dash, dash-dot, dash-dot-dot, and dotted curves are for $N_A/N_B = 1/20, 1/4, 1, 4$, and 20 , respectively.

to the jump appearing at $C_{AB} = C_0$, the asymmetric states become lower in energy once $C_{AB} > C_0$ (i.e., they become the g.s.). This is clearly shown in the figure.

Recalled that the kinetic energy has been neglected. When the particle number is huge, the ratio of the kinetic energy over the total energy is small (say, in an estimation given in [29], the ratio is 6% when $N = 12000$). Thus the neglect will not spoil the qualitative results.

V. THE PHASE-DIAGRAM AGAINST THE INTER- AND INTRA-SPECIES INTERACTIONS

The second type of phase-diagrams are given in Fig.5.

The physics extracted from Fig.5 and from Fig.1 are similar. Therefore, we just mention a few points: (i) The zones for the immiscible phase appear only in the neighborhood of the horizontal line at which $C_{AB} = C_0$. (ii) For all the cases with $C_{AB} \lesssim C_0$, the immiscible and miscible phases are competing. when C_B is much stronger than C_A , the B-atoms will form a shell and the g.s. is in the [A-B] phase. When C_B is not so strong, the B-atoms will be closer to the core and the [A-B] becomes (A,B). When C_B reduces further, the B-atoms will have a narrower distribution while the A-atoms will be distributed more outward, and the (A,B) becomes (B,A). When C_B becomes very weak, the A-atoms will form a shell and the (B,A) becomes [B-A]. (iii) When C_{AB} decreases further from C_0 , immiscible phase disappears.

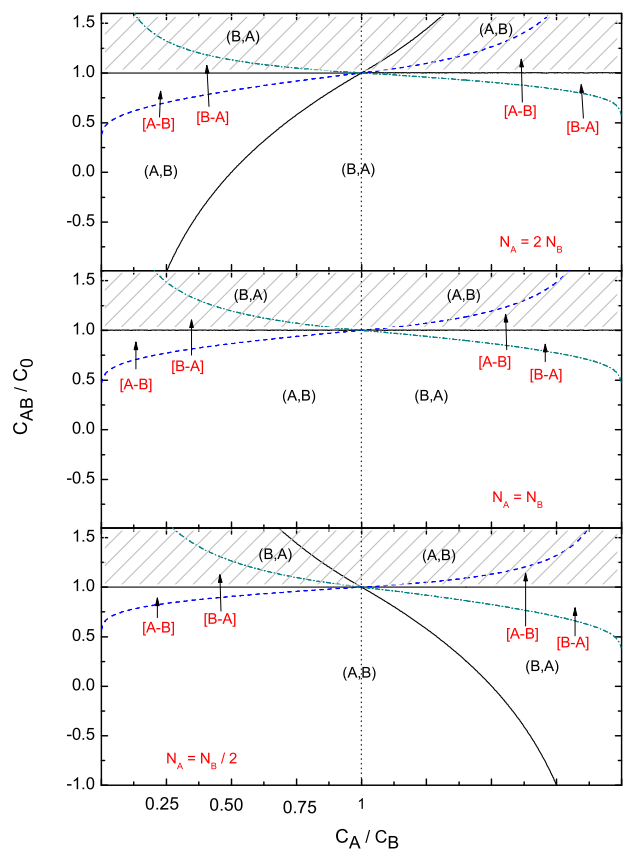


FIG. 5: (Color online) The phase diagram with respect to C_A/C_B and C_{AB}/C_0 . $\gamma_A = \gamma_B = 1$, $N_B = 10^4$, and N_A is given at three values marked in the panels. $C_B = 10^{-3}$. The abscissa x for C_A/C_B is given from 0 to 2. When $x \leq 1$, $C_A/C_B = x$. When $x > 1$, $C_A/C_B = 1/(2-x)$ (in other words, C_A/C_B is ranged from 0 to ∞). Refer to Fig.1.

VI. SUMMARY AND FINAL REMARKS

(i) Due to the introduction of the W-strengths, analytical solutions of the CGP can be expressed in a considerably simpler form to facilitate related analysis.

(ii) A model for the asymmetric g.s. has been proposed. The competition between the symmetric and asymmetric states has been evaluated. A big gap in energy was found during the [A-B] to [B-A] (or reversely) transition which takes place when C_{AB} crosses C_0 . Due to the gap, the asymmetric states become the g.s. once $C_{AB} > C_0$.

It has been known that, in the low-density region, the overlap of the two wave functions will be remarkably underestimated under the TFA. Thus the energy $\langle V_{AB} \rangle$ will be therefore underestimated. This would affect the evaluation of the gap. However, the gap appears only when a kind of atoms tend to leave completely from the other kind. In this case, the percent of $\langle V_{AB} \rangle$ in the total energy is extremely small. Thus, the existence of the gap, which is the difference of the two total energies, will not be spoiled by using the TFA.

(iii) The whole parameter-space has been divided into zones each supports a specific spatial configuration. Based on the division two types of phase-diagrams have been plotted. Making use of the phase-diagrams where the boundaries have analytical forms, the effects of various parameters can be clarified not only qualitatively but also quantitatively.

(iv) Additional effort is made to study the feature of the g.s. when $C_{AB} \lesssim C_0$ and $C_{AB} \gtrsim -C_0$. In the former case the shell tends to separate from the core completely, while in the latter the system tends to collapse.

(v) We have found a critical point $(C)_{crit}$ which is also useful in application. One can tune N_A and/or ω_A to make $(C)_{crit}$ tends to 1 to prohibit the formation of a shell (i.e., the shell can not be formed even if C_{AB} is sufficiently strong), or to make $(C)_{crit}$ differs remarkably from 1 to facilitate the formation of a shell (i.e., the shell can be formed even if C_{AB} is rather weak).

The point $(C)_{crit}$ is associated with the case that a kind of atoms tend to leave completely from the center. In this case TFA is still applicable in the qualitative sense (comparing Fig.1b and 1c of [28], where 1b is closer to the above case).

(vi) We have found another critical point $(N_A/N_B)_{crit}$ which marks the complete overlap of u/r and v/r . This finding has potential usage. In experiments, one can tune the tunable parameters (say, the trap frequency and/or the strengths) so that the two density profiles overlap. Then, once all the other parameter are known, N_A/N_B can be directly known from eq.(6). Since the particle numbers are in general difficult to determine precisely, this approach provides an auxiliary way helpful for determining the numbers.

It was found that in the case that both u/r and v/r are nonzero at $r = 0$ and close to each other, the TFA wave functions deviate very slightly from those beyond the TFA (comparing Fig.1a and 1b of [28]). Therefore, eq.(6) is reliable because it is just associated with this case.

Acknowledgments

Supported by the National Natural Science Foundation of China under Grants No.11372122, 11274393, 11574404, and 11275279; the Open Project Program of State Key Laboratory of Theoretical Physics, Institute of Theoretical Physics, Chinese Academy of Sciences, China; and the National Basic Research Program of China (2013CB933601).

Appendix: Analytical solutions of the CGP under TFA and a division of the parameter-space

A. Miscible phase

For the miscible phase (A,B), the normalized solutions u and v are distributed in two domains of r . In the first domain ($0 \leq r \leq (\frac{15}{2Y_1})^{1/5} \equiv r_a$) they appear as

$$u^2/r^2 = X_1 - Y_1 r^2 \quad (14)$$

$$v^2/r^2 = X_2 - Y_2 r^2 \quad (15)$$

where Y_1 and Y_2 are defined in eq.(5) depending on the W-strengths directly,

$$X_1 = (15/2)^{2/5} Y_1^{3/5} \quad (16)$$

$$\varepsilon_2 = \frac{1}{2} [15(\alpha_2 + \beta_2)]^{2/5} \quad (17)$$

$$X_2 = (\varepsilon_2 - \beta_2 X_1)/\alpha_2 \quad (18)$$

Furthermore, when X_1 and X_2 are known, ε_1 is related to them as $\varepsilon_1 = \alpha_1 X_1 + \beta_1 X_2$.

In the second domain ($r_a < r \leq \sqrt{2\varepsilon_2}$)

$$u^2/r^2 = 0 \quad (19)$$

$$v^2/r^2 = \frac{1}{\alpha_2} (\varepsilon_2 - r^2/2) \quad (20)$$

when $r > \sqrt{2\varepsilon_2}$, both u and v are zero. Thus r_a and $\sqrt{2\varepsilon_2}$ mark the outward borders of the A-atoms and B-atoms, respectively. One can check directly that the above u and v satisfy the CGP, they are normalized, and they are continuous at the common border of the domains (however their derivatives are not).

Obviously, the above solution would be physically meaningful only if the W-strengths are so preset that $Y_1 > 0$, $\alpha_2 + \beta_2 > 0$, and $\sqrt{2\varepsilon_2} > r_a$. The latter can be satisfied when $Y_1 \geq Y_2$ is preset. Besides, in order to have both u/r and v/r being ≥ 0 at $r = 0$, $X_2 \geq 0$ (or $\varepsilon_2 > \beta_2 X_1$, equivalently $[2(\alpha_2 + \beta_2)Y_1]^{2/5} \geq 2\beta_2 Y_1$) is required. Due to this constraint, the phase (A,B) could emerge only in a specific zone inside the whole parameter-space. This zone is bound by the surfaces $Y_1 = Y_2$ and $X_2 = 0$. Inside this zone $Y_1 > 0$, $Y_1 \geq Y_2$, and $X_2 > 0$ hold. Referred to Fig.1 and 5.

For attractive V_{AB} , $X_2 > 0$ holds always. Thus the border $X_2 = 0$ does not appear. Accordingly, the zone for (A,B) is bound by the surfaces $Y_1 = Y_2$ and $C_{AB} = -C_0$ (where $C_0 \equiv \sqrt{C_A C_B}$). However, when $C_{AB} \rightarrow -C_0$ or $\alpha \rightarrow 0$, both Y_1 and Y_2 tend to $+\infty$. Hence, r_a becomes extremely small and the system is highly dense at the center. This will lead to a collapse. Due to the collapse, the case $C_{AB} \leq -C_0$ is not considered.

For (B,A), the solution can be similarly obtained from the above formulae by an interchange of u and v together with an interchange of the indexes 1 and 2. Thus, associated with the zone for (A,B), there is a partner-zone for (B,A), where the A- and B-atoms interchange their role.

B. Immiscible phase

For $[A - B]$, u and v are distributed in three domains $(0, r_b)$, (r_b, r_c) , and $(r_c, \sqrt{2\varepsilon'_2})$, where

$$r_c^5 = \frac{15\alpha_1\alpha_2}{2\alpha Y_1}(1 + \frac{\beta_1}{\alpha_1}(1 - \mathfrak{C})) \quad (21)$$

$$r_b^5 = -\frac{15\alpha_1\alpha_2}{2\alpha Y_2}(1 + \frac{\beta_2}{\alpha_2} - \mathfrak{C}) \quad (22)$$

and \mathfrak{C} satisfies the following equation

$$15\alpha_2\mathfrak{C} = (2\beta_2 Y_1 r_c^2 + 2\alpha_2 Y_2 r_b^2)^{5/2} \quad (23)$$

When this equation has been solved \mathfrak{C} can be obtained. If \mathfrak{C} ensure that the right sides of eqs.(21,22) are positive, we can obtain r_c , r_b .

Then, in the first domain $(0, r_b)$

$$u^2/r^2 = \frac{1}{\alpha_1}(\varepsilon'_1 - r^2/2) \quad (24)$$

$$v^2/r^2 = 0 \quad (25)$$

where

$$\varepsilon'_1 = \alpha_1 r_c^2 Y_1 + \beta_1 r_b^2 Y_2 \quad (26)$$

In the second domain (r_b, r_c)

$$u^2/r^2 = Y_1(r_c^2 - r^2) \quad (27)$$

$$v^2/r^2 = Y_2(r_b^2 - r^2) \quad (28)$$

In the third domain $(r_c, \sqrt{2\varepsilon'_2})$

$$u^2/r^2 = 0 \quad (29)$$

$$v^2/r^2 = \frac{1}{\alpha_2}(\varepsilon'_2 - r^2/2) \quad (30)$$

where

$$\varepsilon'_2 = \frac{1}{2}(15\alpha_2\mathfrak{C})^{2/5}. \quad (31)$$

Since u^2/r^2 and v^2/r^2 should be positive in the second domain, $Y_1 > 0$ and $Y_2 < 0$ are both necessary. In particular, the latter condition $Y_2 < 0$ assures the emergence of the shell formed by the B-atoms (because a negative Y_2 assures that v/r increases with r as shown in eq.(28)). Note that, for attractive V_{AB} , we know from the definitions of Y_1 and Y_2 that they must have the same sign. Thus the immiscible phase does not exist when the interspecies interaction is attractive (refer to Fig.1 and 5). Therefore, C_{AB} is considered as positive in the follows.

Obviously, $0 \leq r_b \leq r_c \leq \sqrt{2\varepsilon'_2}$ is further required to assure that the solution is meaningful. When $\alpha > \mathbf{0}$ and with the preset $Y_1 > 0$ and $Y_2 < 0$ the condition $r_b \geq 0$ can be satisfied if $\mathfrak{C} \leq 1 + \frac{\beta_2}{\alpha_2}$. Besides, from eqs.(21,22) we have

$$r_c^5 - r_b^5 = \frac{15\alpha_2\alpha}{(\alpha_1 - \beta_2)(\alpha_2 - \beta_1)}(\frac{\alpha_1}{\alpha_2} + 1 - \mathfrak{C}) \quad (32)$$

Thus the condition $r_c \geq r_b$ can be satisfied if $\mathfrak{C} \geq 1 + \frac{\alpha_1}{\alpha_2}$. Furthermore, from eq.(31) and making use of eq.(23), we have $2\varepsilon'_2 = 2\beta_2 Y_1 r_c^2 + 2\alpha_2 Y_2 r_b^2$. Note that, from eq.(5) we have

$$2\alpha_2 Y_2 + 2\beta_2 Y_1 = 1 \quad (33)$$

Then, $2\varepsilon'_2 = r_c^2 - 2\alpha_2 Y_2(r_c^2 - r_b^2)$. Thus, when Y_2 is negative and $r_c \geq r_b$ holds, the condition $\sqrt{2\varepsilon'_2} \geq r_c$ is satisfied. To conclude, if we can find out a \mathfrak{C} satisfies eq.(23) and is lying in the range $1 + \frac{\alpha_1}{\alpha_2} \leq \mathfrak{C} \leq 1 + \frac{\beta_2}{\alpha_2}$, then the u and v given above is a physically meaningful solution. By solving eq.(23) numerically, a unique \mathfrak{C} ranging inside the above range

can be found. Thus, we obtain the solution for the immiscible phase.

Let us find out the zone in the parameter-space that supports the $[A - B]$ solution. When $\mathfrak{C} = 1 + \frac{\beta_2}{\alpha_2}$, we have $r_b = 0$, $r_c = \sqrt{X_1/Y_1} \equiv r_a$, and $\varepsilon'_2 = \varepsilon_2$. Thus the wave functions of the $[A - B]$ and those of (A,B) with $X_2 = 0$ overlap. Recall that $X_2 = 0$ is a border of (A,B). Thus the zone of $[A - B]$ is adjacent to the zone of (A,B), and they have the common border $X_2 = 0$.

When $C_{AB} \rightarrow C_0$ (or $\alpha \rightarrow \mathbf{0}$), we know from eq.(32) that $r_b \rightarrow r_c$, thus the shell tends to separate from the core completely. Examples are shown in Fig.3. Since $r_b > r_c$ is not allowed, $\alpha = \mathbf{0}$ should be the other border. Note that, when $\alpha = \mathbf{0}$, the CGP has no physical solution. Thus, a complete separation between the shell and the core is not allowed. To conclude, the zone of $[A - B]$ requires $Y_1 > 0$ and $Y_2 < 0$ and is bound by the borders $X_2 = 0$ and $\alpha = \mathbf{0}$.

The case with $\alpha < \mathbf{0}$ is associated with metastable states, they can be similarly discussed, if necessary. The partner zone of $[A - B]$, namely, $[B - A]$, can be similarly obtained by interchanging u and v , and interchanging the indexes 1 and 2.

[1] T.L.Ho and V.B.Shenoy, *Phys. Rev. Lett.* **77**, 3276 (1996).

[2] C.J.Myatt, E.A.Burt, R.W.Ghrist, E.A.Cornell and

- C.E.Wieman, *Phys. Rev. Lett.* **78**, 586 (1997).
- [3] C.Ospelkaus, *et al.*, *Phys. Rev. Lett.* **97**, 120402 (2006).
- [4] C.Weber, *et al.*, *Phys. Rev. A* **78**, 061601(R) (2008).
- [5] K.-K.Ni, *et al.*, *Science* **322**, 231 (2008).
- [6] M.Baranov, *Phys. Rep.* **464**, 71 (2008).
- [7] M.Anderlini, *et al.*, *Phys. Rev. A* **71**, 061401(R) (2005).
- [8] K.Pilch, *et al.*, *Phys. Rev. A* **79**, 042718 (2009)
- [9] N.Nemitz, F.Baumer, F.Münchow, S.Tassy and A.Görlitz, *Phys. Rev. A* **79** 061403 (2009) .
- [10] L.Wacker, *et al.*, *Phys. Rev. A* **92**, 053602 (2015)
- [11] B.D.Esry, C.H.Greene, J.P.Burke, J.L.Bohn, *Phys. Rev. Lett.* **78**, 3594 (1997).
- [12] H.Pu and N.P.Bigelow, *Phys. Rev. Lett.* **80**, 1130 (1998).
- [13] E.Timmermans, *Phys. Rev. Lett.* **81**, 5718 (1998).
- [14] P.Ao and S.T.Chui, *Phys. Rev. A* **58**, 4836 (1998).
- [15] S.T.Chui and P.Ao, *Phys. Rev. A* **59**, 1473 (1999).
- [16] M.Trippenbach, K.Goral, K.Rzazewski, B.Malomed, and Y.B.Band, *J.Phys.B:At.Mol.Phys.* **33**, 4017 (2000).
- [17] F.Riboli and M.Modugno, *Phys. Rev. A* **65**, 063614 (2002).
- [18] A.A.Svidzinsky and S.T.Chui, *Phys. Rev. A* **67**, 053608 (2003).
- [19] M.Luo, Z.B.Li and C.G.Bao, *Phys. Rev. A* **75**, 043609 (2007).
- [20] Z.F.Xu, Y.Zhang, and L.You, *Phys. Rev. A* **79**, 023613 (2009)
- [21] Y.Shi and L.Ge, *Phys. Rev. A* **83**, 013616 (2011).
- [22] S.Gautam and D.Angom, *J.Phys.B:At.Mol.Phys.* **43**, 095302 (2010).
- [23] P.N.Galteland, E.Babaev, and A.Sudbø, *New J. Phys.* **17** 103040 (2015) .
- [24] B.VanSchaeybroeck and J.O.Indekeu, *Phys. Rev. A* **91**, 013626 (2015).
- [25] J.O.Indekeu, C.Y.Lin, N.Van Thu, B.Van Schaeybroeck, and T.H.Phat, *Phys. Rev. A* **91**, 033615 (2015).
- [26] A.Roy and D.Angom, *Phys.Rev. A* **92**, 011601(R) (2015).
- [27] M.Luo, C.G.Bao, and Z.B.Li, *J.Phys.B: At.Mol.Opt.Phys.* **41**, 245301(2008).
- [28] J.Polo, *et al.*, *Phys. Rev. A* **91**, 053626 (2015).
- [29] Y.Z.He, Y.M.Liu, and C.G.Bao *Phys. Rev. A* **91**, 033620 (2015).